Supporting Information for

Achieving the Ratiometric Imaging of Steroid Sulfatase in Living Cells and Tissues with a Two-Photon Fluorescent Probe

Wei Li,[a] Shulu Yin,[a] Xiangyang Gong,[a] Wang Xu,[a] Ronghua Yang,[b] Yichao Wan,[c] Lin Yuan,*[a] XiaoBing Zhang[a]

[a] *State Key Laboratory of Chemo/Biosensing and Chemometrics, College of Chemistry and Chemical Engineering, Hunan University, Changsha 410082, China*

[b] *School of Chemistry and Biological Engineering, Changsha University of Science and Technology, Changsha, China*

[c] *Key Laboratory of Theoretical Organic Chemistry and Functional Molecule (MOE), College of Chemistry and Chemical Engineering, Hunan University of Science and Technology, Xiangtan 411201, China*

China E-mail: lyuan@hnu.edu.cn (L. Y)

Table of Contents:

1. Materials and General Experimental Methods

Reagents and apparatus. All chemical reagents used in synthesis were supplied from the commercial purchaser without purification unless otherwise stated, and solvents used were purified by standard methods prior to use. The water used in the whole experiment was twice-distilled water. Sulfatase (from Helix pomatia S9626, and from aerobacter aerogenes S1629) and STX64 were purchased from Sigma-Aldrich. Ultrapure water (over 18 MΩ·cm) was used throughout the experiments. ^{1}H NMR and ^{13}C NMR spectra were recorded on a Bruker-400 spectrometer with TMS acting as an internal standard. Mass spectra were performed from an LCQ Advantage ion trap mass spectrometer (Thermo Finnigan) and ESI/Q-TOF Micro TM HRMS High-resolution electron spray (Zhengzhou University Analysis and Testing Center). Absorption and fluorescence spectroscopic studies were performed in a UV-1800 ultraviolet and visible spectrophotometer (Shimadzu Corporation, Japan) and a Hitachi F-4600 fluorescence spectrophotometer. The pH measurements were carried out on a PHS-3C pH meter (INESA instruments). One-photon and two-photon fluorescence imaging were performed on Nikon A1 plus confocal microscope (Nikon, Japan). TLC analysis was performed on silica gel plates and column chromatography was conducted over silica gel (mesh 200-300) columns, both of which were obtained from the Yantai Jiangyou Silica Gel Development Company Limited.

Determination of the fluorescence quantum yield. Fluorescence quantum yield for **ERNathS** and **ERNathOH** was determined by using coumarin 102 (Φ_f = 0.93 in EtOH) or Rhodamine B (Φ_f = 0.65 in EtOH) as a fluorescence standard.[1, 2] The quantum yield was calculated using the following equation:

$$\Phi_s = \Phi_r \, (Ar \, F_s / A_s \, F_r) \, (n_s^2 / n_r^2)$$

Where, *s* and *r* denote sample and reference, respectively. *A* is the absorbance at the excitation wavelength. *F* is the relative integrated fluorescence intensity and *n* is the refractive index of the solvent. Φ is the fluorescence quantum yield.

Measurement of two-photon absorption cross section. The two-photon excited fluorescence intensity of **ERNathS** and **ERNathOH** were measured at 710-840 nm using Rhodamine B in MeOH as the reference [3]. **ERNathS** and **ERNathOH** were dissolved in a Tris-HCl/DMSO buffer solution (50 mM, pH 7.0, Tris/DMSO = 7: 3, v/v). The TP absorption cross-section (δ) was calculated using the following equation:

$$\delta = \delta_r \, (F_s \, n_s^2 \, \phi_r \, C_r) \, / \, (F_r \, n_r^2 \, \phi_s \, C_s)$$

where, *s* and *r* denote sample and reference, respectively. *F* is the average fluorescence intensity, *n* is the refractive index of the solvent, *C* is the concentration, Φ is the quantum yield, and δ_r is the two-photon cross-section of the reference molecule.

Detection limit calculation. The detection limit was calculated based on the fluorescence titration. The detection limit is calculated using the following equation:

$$\text{Detection limit} = 3\sigma / k$$

where σ is the standard deviation of blank measurements, *k* is the slope between the fluorescence ratios versus sample concentration.

Density functional theory (DFT) calculation. The ground state structure of compounds **ERNathS** and **ERNathO**$^-$ were optimized using DFT with B3LYP function and 6-31G* basis set,[4, 5] and using a CPCM solvation model with water as the solvent. And the excitation energies of **ERNathS** and **ERNathO**$^-$ in quantum chemistry were calculated by the most popular method time

dependent density functional theory (TD-DFT).[6] All of these calculations were performed with Gaussian 09 program package.[7]

Molecule docking. Docking simulation was performed by using SYBYL (X-2.1). Here, the X-ray crystallographic structure of human arylsulfatase (PDB entry 1E2S [8]) was selected for docking analysis. The structure of the probe **ERNathS** was assigned with Gasteiger-Huckel charges. Other parameters not mentioned were set at default values. Based on a 2-hydroxy-5-nitrophenyl sulphate-based ligand complexed with the crystal structure of 1E2S, the bioactive binding site was generated using Surflex-Dock.

Procedure for spectra experiments. Absorption spectra and emission spectra were both measured in Tris-HCl buffer with an excitation wavelength at 405 nm. In experiment group, the sulfatase was incubated with probe **ERNathS** *in vitro* at 37 °C for 60 min, and the mixtures was transferred to a 3 cm quartz cell to test its absorbance or fluorescence intensity with an excitation wavelength at 405 nm. As a control group without adding sulfatase, the test conditions are consistent with the experiment group.

Cell cytotoxicity in MTT assay. Cells were plated in 96-well flat-bottomed plates at 1×10^5 cells per well and allowed to grow overnight prior to exposure to **ERNathS** with different concentrations. Then the MTT (0.5 mg/mL) reagent was added for 4 h at 37 °C and DMSO (100 μL/well) was further incubated with cells to dissolve the precipitated formazan violet crystals at 37 °C for 15 min. The absorbance was measured at 490 nm by a multi-detection microplate reader. The following formula was used to calculate the viability of cell growth: Cell viability (%) = (mean of A value of treatment group - mean of A value of control) × 100.

Fluorescence microscopic imaging. All cell imaging experiments were conducted in living cells. In experiment group, cells were incubated with **ERNathS** (20 μM) for 2 h at 37 °C then washed with DPBS three times prior to imaging. The control group were pre-treated with 20 μM STX64 (the inhibitor of sulfatase) for 2 h and washed three times with DPBS, and then incubated with **ERNathS** under the same condition. Tumor tissue slices of 400 μm thickness were prepared from a tumor-bearing 3-weeks female BALB/c mice and incubated with 40 μM **ERNathS** in DPBS for 4 h at 37 °C, then washed with DPBS prior to imaging. In experiment group, the tumor tissue slices were pretreated with STX64 for 2 h and treated with 40 μM **ERNathS** for 4 h at 37 °C before imaging. In the control group, the normal tissue slices were taken from normal mouse breast tissues and then treated with 40 μM **ERNathS** under same condition for comparison. The fluorescence confocal imaging was performed using Nikon A1 plus confocal microscope with a 10× or 40× water objective. The fluorescence images were captured from the blue channel of 425-475 nm and green channel of 500-550 nm with an one-photon excitation at 405 nm or two-photon excitation at 820 nm. 3-dimensional (3D) imaging was captured with the z-stack mode of the microscope under two-photon excitation.

Determination of STS in cells by ELISA kit

The cell lysate was prepared according to the following procedure. In a test tube, 10×10^5 cells (HEK-293 HL-7702, HepG-2, HeLa or MCF-7 cells) in 1 mL DMEM was centrifugated at 1000 rpm for 5 min, and then the supernatant was discarded, followed by washing the cells with PBS for three times. It was then placed at -20 °C overnight. After two times of repeated freezing and thawing to destroy the cell membrane, the tube was centrifugated at 5000 rpm for 5 min at 2-8 °C, and the supernatant was collected for use. The concentration of STS in cells was determined by measuring the absorbance at 450 nm using a commercial RD 48T ELISA kit. Briefly, to each well,

50 μL samples or 100 μL standards, and 50 μL enzyme marked reagents were mixed. After incubating the reaction mixture at 37 °C for 60 min, the wells were washed five times with washing solution, and then 50 μL chromogen reagents A and B were added into the wells in succession, followed by incubating in the dark for 15 min at 37 °C. Finally, 50 μL stop buffer was added to the wells, and the absorbance of each well was recorded at 450 nm on a Microtiter Plate assay system. The standard curve for STS detection was constructed following the direction of the kit in the concentration range from 0 to 900 pg/mL, and the corresponding concentrations were calculated according to the standard curve. Data are expressed as mean ± standard deviation of three separate measurements.

Visualization of STS activity in tissues of mice xenograft tumor model

All procedures procedures were carried out in accordance with the Guidelines for Care and Use of Laboratory Animals of Hunan University, and were approved by the Animal Ethics Committee of College of Biology (Hunan University). For establishing a mouse tumor model, the 4T1 mammary carcinoma cells were chose to transplant of approximately 20 g female BALB/c mice. After three-weeks inoculation, the xenograft tumor mice were sacrificed, and got various fresh tissues.

Statistical analysis

All data are expressed as the mean of three separate experiments. Statistical significance were analyzed with unpaired two-tailed Student's t-tests. *P ≤ 0.05, **P ≤ 0.01. ***P ≤ 0.001.

2. Synthesis and Characterization

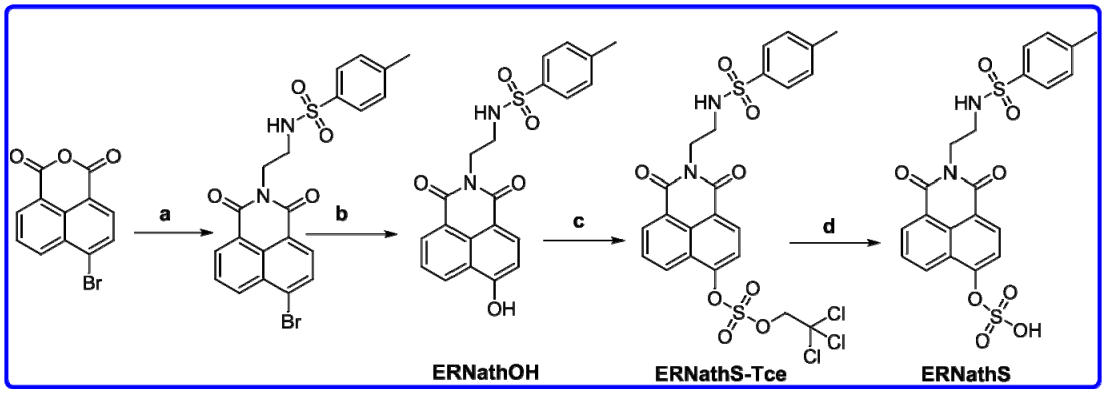

Scheme S1. Synthetic routes of the probe **ERNathS**

Synthesis of 1b

Compound **1b** was synthesized according to a literature procedure.[9]

Synthesis of ERNathOH

The compound **1b** (1.0 mmol, 472.6 mg), N-hydroxysuccinimide (2.0 mmol, 320.7 mg) and K_2CO_3 (3.0 mmol, 396.2 mg) was dissolved in 25 mL DMSO. The mixture was heated to 80 °C for 12 h. When the mixture was cooled to room temperature, the mixture was poured onto ice and neutralized with dilute hydrochloric acid to pH = 7.0. Then the resulting precipitate was filtered off and purified by silica gel column chromatography to give a yellow solid **ERNathOH** (315.7 mg, 77.1 %). ^{1}H NMR (400 MHz, DMSO) δ 8.50 (t, *J* = 9.5 Hz, 1H), 8.41 (d, *J* = 7.2 Hz, 1H), 8.28 (t, *J* = 10.1 Hz, 1H), 7.74 – 7.70 (m, 1H), 7.58 (t, *J* = 8.2 Hz, 2H), 7.20 (t, *J* = 9.3 Hz, 2H),

7.13 (d, J = 8.2 Hz, 1H), 4.08 (t, J = 6.5 Hz, 2H), 3.06 (dd, J = 12.9, 6.4 Hz, 2H), 2.23 (d, J = 17.2 Hz, 3H). ^{13}C NMR (100 MHz, DMSO) δ 164.2, 163.5, 161.0, 142.9, 138.1, 134.0, 131.5, 129.9, 129.8, 129.3, 126.8, 125.9, 122.9, 122.3, 112.9, 110.4, 40.9, 39.4, 21.3. MS (ESI): m/z [M-H$^-$] = 409.1.

Synthesis of ERNathS

First, the compound **ERNathOH** (0.5 mmol, 214.2 mg), 200 μL Et_3N and DMAP (0.6 mmol, 70.5 mg) was dissolved in dry CH_2Cl_2/MeCN (v/v = 8/3, 11 mL) and the mixture was stirred at ice bath under argon atmosphere for10 min. Then, trichloroethylsulfuryl chloride (300 μL) was introduced to the mixture via a syringe and the reaction mixture was stirred at room temperature for 12 h. The mixture was concentrated under vacuum, and the residue was purified by silica chromatography eluted with CH_2Cl_2/petroleum (2:1, v/v) to afford compound **ERNathS-Tce** as an white solid (115.2 mg, 37.2 %). ^{1}H NMR (400 MHz, $CDCl_3$) δ 8.51 (d, J = 7.2 Hz, 1H), 8.47 (d, J = 8.1 Hz, 1H), 8.41 (d, J = 8.4 Hz, 1H), 7.80 (dd, J = 15.9, 7.9 Hz, 2H), 7.47 (d, J = 7.6 Hz, 2H), 6.76 (d, J = 7.6 Hz, 2H), 4.91 (s, 2H), 4.20 (s, 2H), 3.38 (d, J = 4.6 Hz, 2H), 1.96 (s, 3H). ^{13}C NMR (100 MHz, $CDCl_3$) δ 164.0, 163.4, 150.1, 142.9, 136.9, 132.5, 131.7, 129.4, 129.3, 128.3, 127.8, 126.7, 124.5, 122.4, 121.5, 118.1, 92.0, 80.9, 42.1, 39.4, 21.2.

Second, the compound **ERNathS-Tce** (0.16 mmol, 100.3 mg), Zn dust (1.0 mmol, 68.6 mg) and $HCOONH_4$ (0.3 mmol, 20.6 mg) was dissolved in CH_2Cl_2/MeOH (v/v = 2/10, 12 mL) and the mixture was stirred at room temperature for 3 h. Then the resulting precipitate was filtered off and the filtrate was concentrated under vacuum, then purified by silica gel column chromatography to give a white solid (45.4 mg, 57.9 %). ^{1}H NMR (400 MHz, MeOD) δ 8.64 (d, J = 8.3 Hz, 1H), 8.51 (s, 1H), 8.46 (s, 1H), 7.91 (d, J = 8.0 Hz, 1H), 7.81 (t, J = 7.8 Hz, 1H), 7.48 (d, J = 7.5 Hz, 2H), 6.84 (d, J = 7.5 Hz, 2H), 4.21 (s, 2H), 3.35 (s, 2H), 2.02 (s, 3H). ^{13}C NMR (100 MHz, MeOD) δ 164.4, 163.9, 154.3, 142.9, 137.5, 132.0, 131.1, 129.2, 128.9, 126.3, 126.1, 125.1, 121.9, 117.5, 116.0, 100.0, 40.7, 39.1, 19.9. HRMS (m/z): Cacld for [M-H$^-$]: 489.0432, found: 489.0433 .

3. Supporting Figures and Table

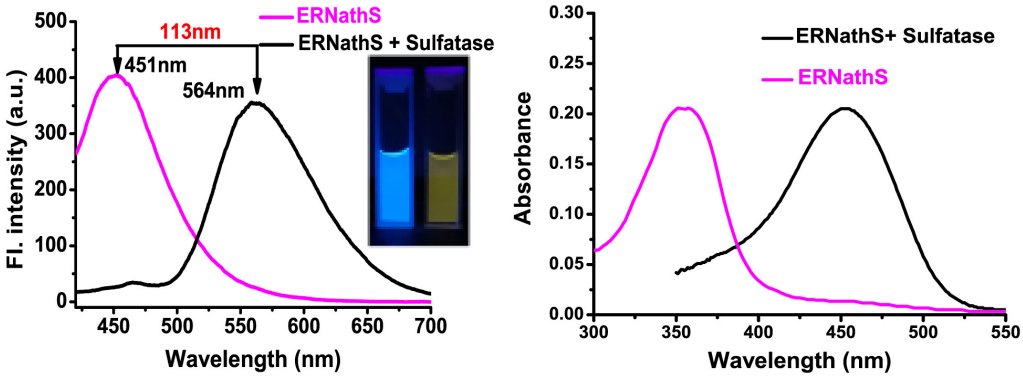

Figure S1. The emission and absorption spectra of **ERNathS** (5 μM) before and after reaction with 0.8 U/mL sulfatase from helix pomatia. The inset shows the fluorescence color change of the solution.

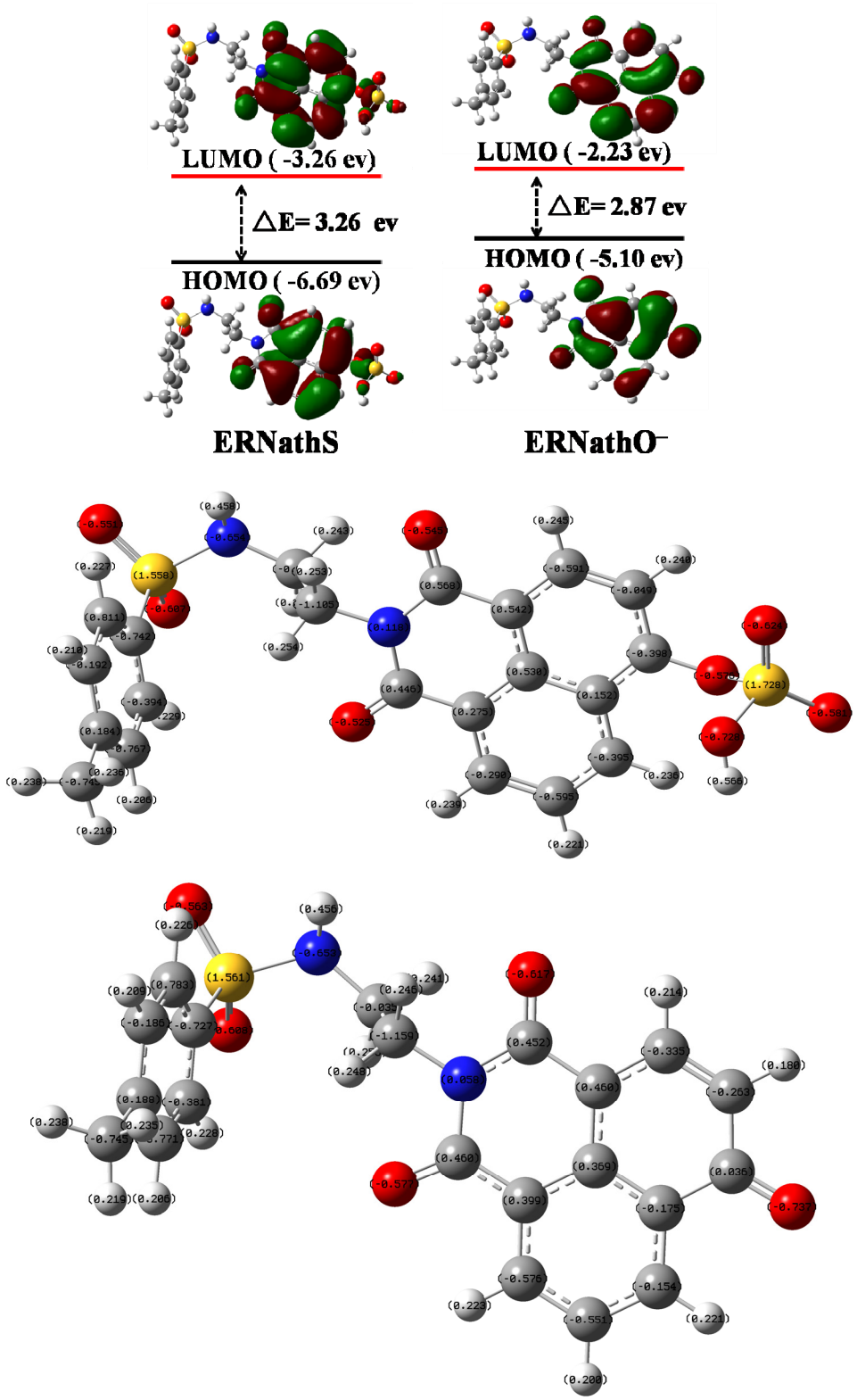

Figure S2. Frontier molecular orbital profiles and the charges of **ERNathS** and **ERNathO**$^{-}$ in the excited states based on DFT (B3LYP/6-31G*) calculations.

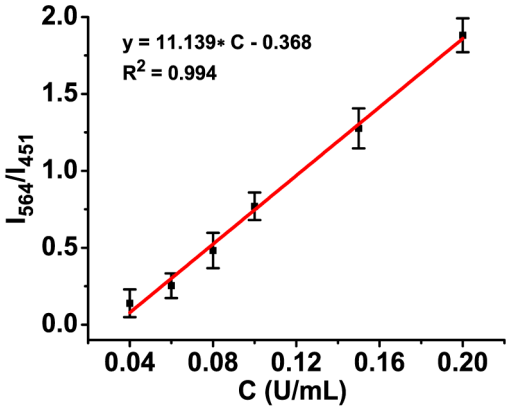

Figure S3. Linear fitting curve of the fluorescence ratio (I_{564}/I_{451}) towards the concentration of sulfatase from 0-0.2 U/mL.

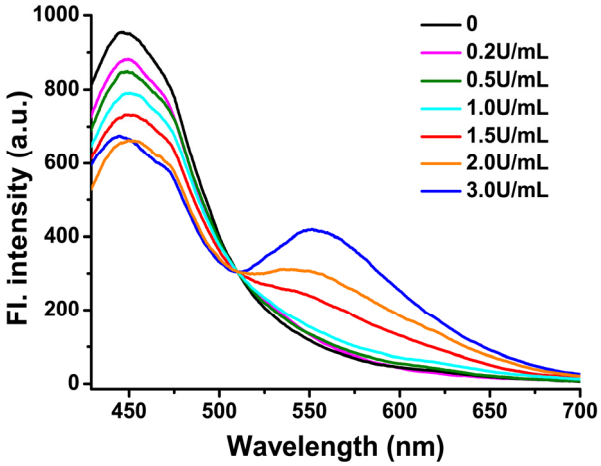

Figure S4. The emission spectra of **ERNathS** (5 μM) after 5 h upon treatment with increasing concentrations of sulfatase (0-3 U/mL) from aerobacter aerogenes in 50 mM Tris-HCl buffer (pH = 7.0, 1% DMSO). λ_{ex} = 405 nm.

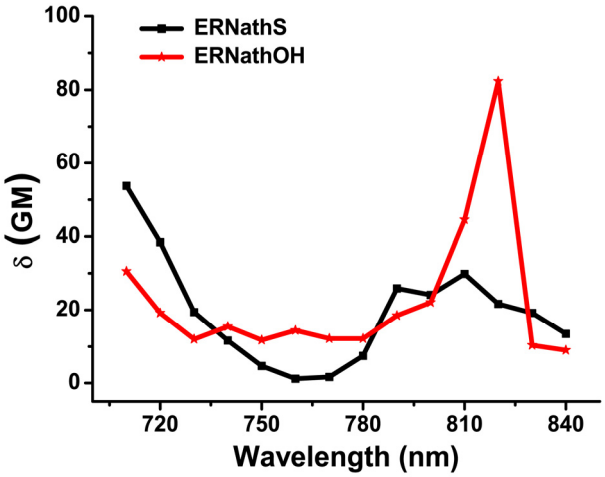

Figure S5. Two-photon absorption cross-section of **ERNathS** and **ERNathOH.**

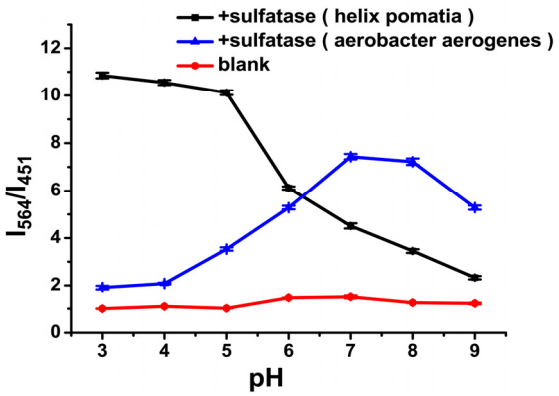

Figure S6. pH-dependent fluorescence ratio (I_{564}/I_{451}) changes of **ERNathS** (5 μM) toward sulfatase from helix pomatia (0.8 U/mL) and aerobacter aerogenes (3 U/mL), respectively. Data are expressed as mean ± SD of three parallel experiments. λ_{ex} = 405 nm.

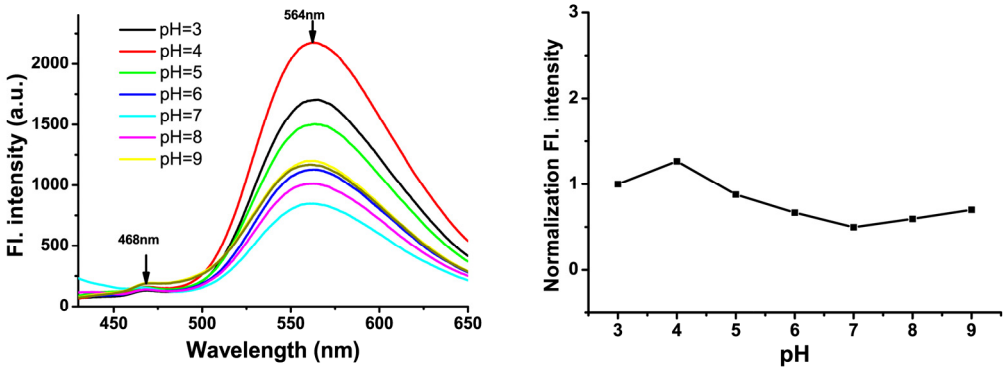

Figure S7. pH-dependent fluorescence intensity changes of **ERNathOH** (5 μM) in 50 mM Tris-HCl buffer at 37 °C. λ_{ex} = 405 nm.

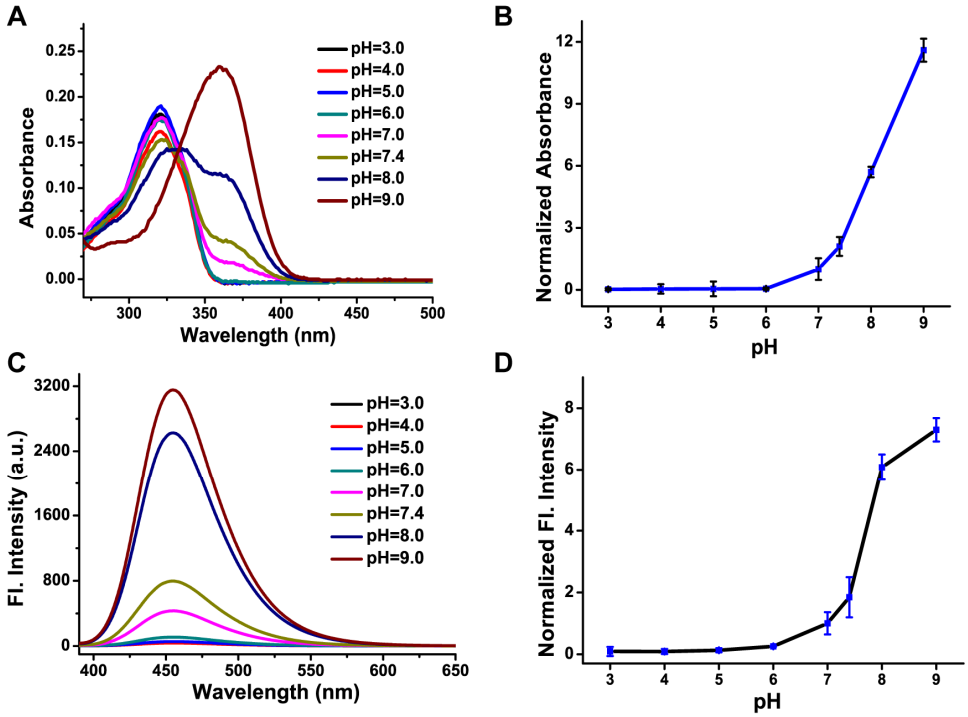

Figure S8. (A) pH-dependent absorption changes of **4-MU** (5 μM) in 50 mM Tris-HCl buffer at 37 °C, (B) The normalized absorbance of **4-MU** at 361 nm in Tris-HCl buffer with pH changing from 3.0 to 9.0. (C) pH-dependent fluorescence intensity changes of **4-MU** (5 μM) in 50 mM Tris-HCl buffer at 37 °C, (D) The normalized fluorescence

intensity of **4-MU** at 454 nm in Tris-HCl buffer with pH changing from 3.0 to 9.0. λ_{ex} = 360 nm.

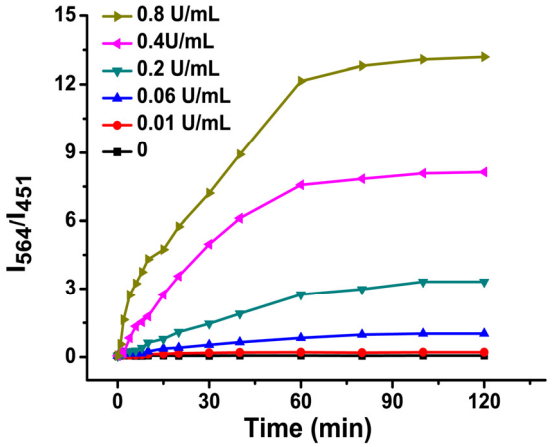

Figure S9. Effects of reaction time on the fluorescence ratio (I_{564}/I_{451}) of **ERNathS** (5 μM) in the presence of varied concentrations of sulfatase (0-0.8 U/mL) from helix pomatia. The reaction was performed at 37 °C in 50 mM Tris-HCl buffer (pH = 5.0). λ_{ex} = 405 nm.

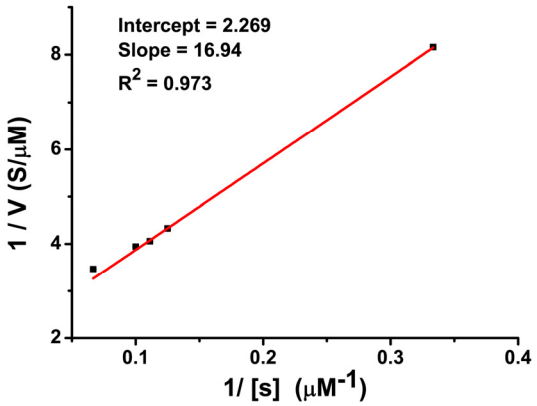

Figure S10. Line weaver-Burk plot for the enzyme-catalyzed reaction. The Michaelis-Menten equation was described as: $V = V_{max}[S] / (K_m + [S])$, where V is the initial reaction rate, $[S]$ (substrate) is the probe **ERNathS** concentration, and the K_m is the Michaelis constant. Conditions: 0.8 U/mL sulfatase, 1-20 μM of **ERNathS**. The measurements were performed at 37 °C with fluorescence ratio I_{564}/I_{451} under the excitation wavelength at 405 nm.

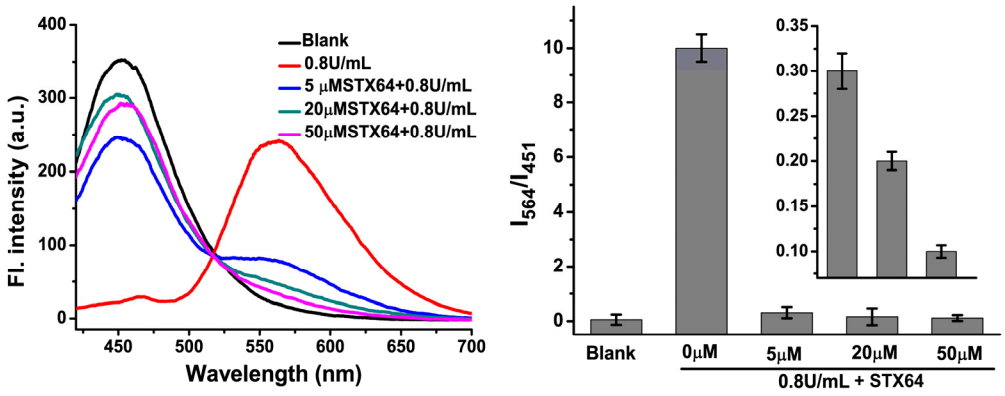

Figure S11. The effects of STX64 at varied concentrations on the emission spectra of **ERNathS** (5 μM). Fluorescence ratio I_{564}/I_{451} of **ERNathS** (5 μM) at 60 min after addition of 0.8 U/mL sulfatase in Tris-HCl buffer (pH = 5.0) with the presence of 0, 5, 20, 50 μM STX64. The inset shows an enlarged of the presence of 5, 20, 50 μM STX64. Data are expressed as mean ± SD of three parallel experiments. λ_{ex} = 405 nm.

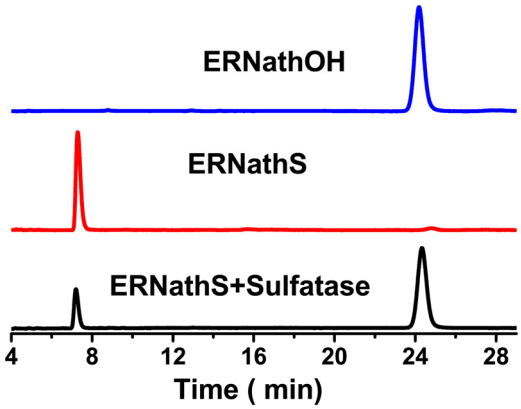

Figure S12. HPLC analysis of reaction products of **ERNathS** with sulfatase. To a solution of **ERNathS** in 50 mM Tris-HCl buffer containing 1% DMSO as a co-solvent, 0.8 U/mL of sulfatase was added, and the reaction mixture was incubated at 37 °C for 60 min. HPLC analysis for **ERNathOH** was performed under an isocratic condition (A: deionized water; B: acetonitrile; A/B = 25/75 for 30 min).

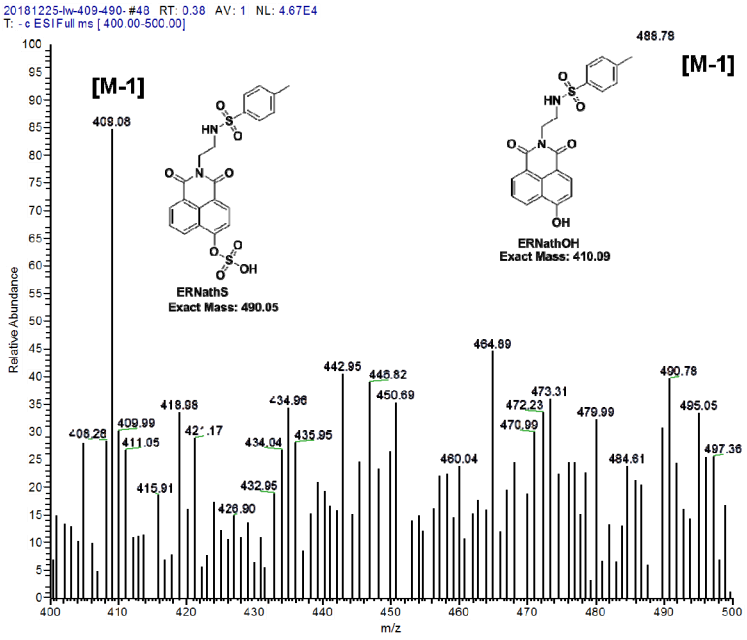

Figure S13. MS spectra showing the analysis of reaction products of **ERNathS** with sulfatase.

Table S1. Representative probes for sulfatase based on organic fluorophore for fluorescence imaging.

Probe	λ_{ex} (nm)	λ_{em} (nm)	Response model	K_m (μM)	Biological application	Reference
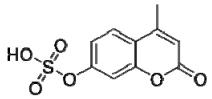 4-MUS	355	460	Turn-on	-	cells lystate and fixed cells	*Anal. Biochem.*, 2003, 318, 276-284
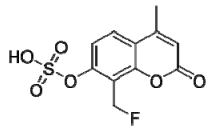 1a	360	450	Turn-on	-	formaldehyde-fixed CHO/STS cells	*Chem. Commun.*, 2014, 50, 6116-6119
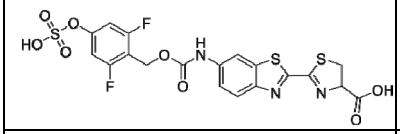	-	522	Turn-on	90.1	HEK293 cells lystate	*ChemBioChem*, 2010, 11, 2096-2099
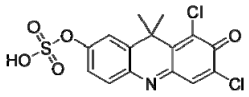 DDAO-sulfate	600	660	Turn-on	13	mycobacterial lysates	*Proc. Natl. Acad. Sci. U. S. A.*, 2013, 110, 12911-12916.
ERNathS	405	564 451	Ratiometric (I_{564}/I_{451})	7.47	various living cells and tissues	*This work*

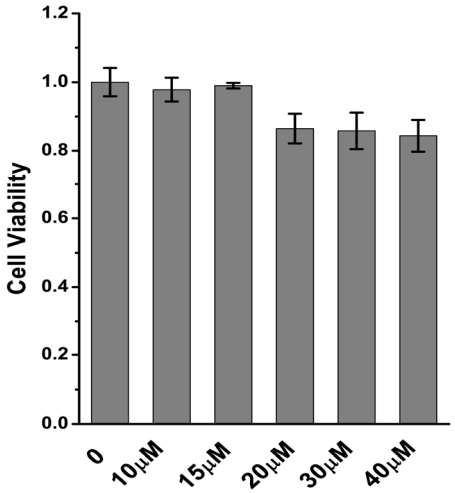

Figure S14. Effects of **ERNathS** with varied concentrations (0-40 μM) on the viability of HepG-2 cells. The viability of the cells without probe is defined as 100%. Data are expressed as mean ± SD of three parallel experiments.

4. Fluorescence Microscopic Studies and Bioanalysis

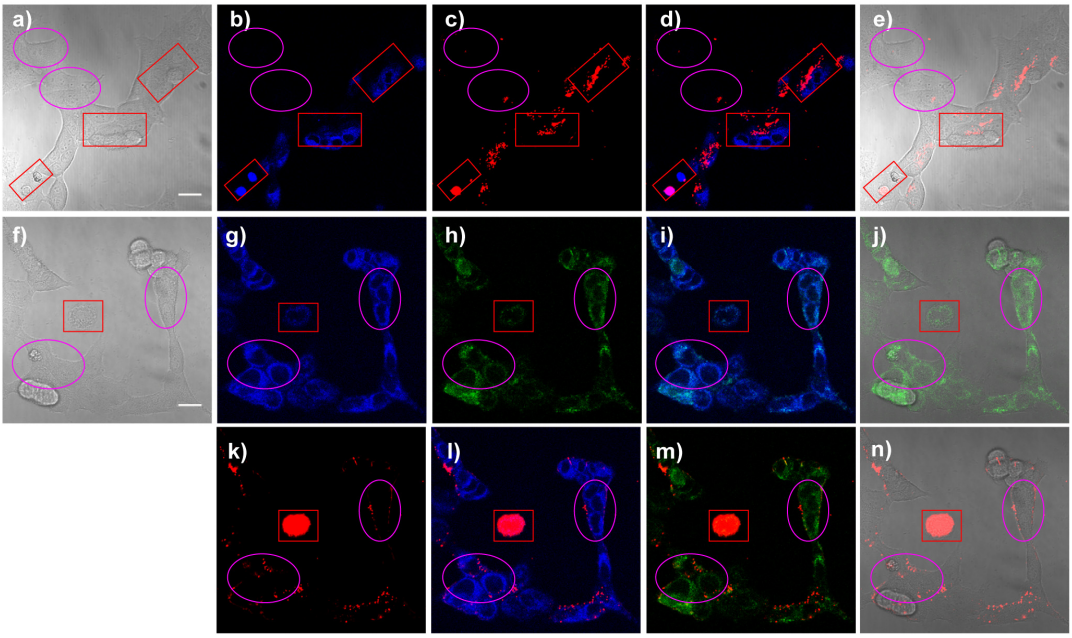

Figure S15. Confocal microscopy images of probe **ERNathS** and commercial probe 4-MUS in live HeLa cells. (a-e): cells were pre-treated with 20 μM 4-MUS for 2 h and then incubated with propidium iodide (PI, 1.5 μM) for 30 min, (a) bright field, (b) blue channel of 4-MUS at 425-475 nm, λ_{ex} = 405 nm. (c) red channel of PI at 570-620 nm, λ_{ex} = 560 nm. (d) the merged image of b and c. (e) the merged image of a and c. (f-n): cells were pre-treated with 20 μM **ERNathS** for 2 h and then incubated with propidium iodide (PI, 1.5 μM) for 30 min, (f) bright field, (g) blue channel of **ERNathS** at 425-475 nm, λ_{ex} = 405 nm. (h) green channel of **ERNathS** at 500-550 nm, λ_{ex} = 405 nm. (i) the merged image of g and h. (j) the merged image of f and h. (k) red channel of PI at 570-620 nm, λ_{ex} = 560 nm. (l) the merged image of g and k. (m) the merged image of h and k. (n) the merged image of f and k. Purple round boxes indicate living cells and well-behaved cells, while red squares indicate dead cells and poorly performing cells. Scale bar: 20 μm.

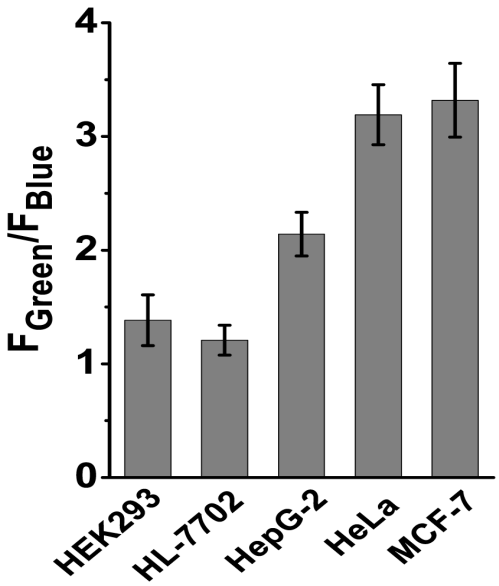

Figure S16. The relative ratio value of fluorescence intensity (F_{Green}/F_{Blue}) in **Fig. 2**. Data represent mean standard error (n = 10).

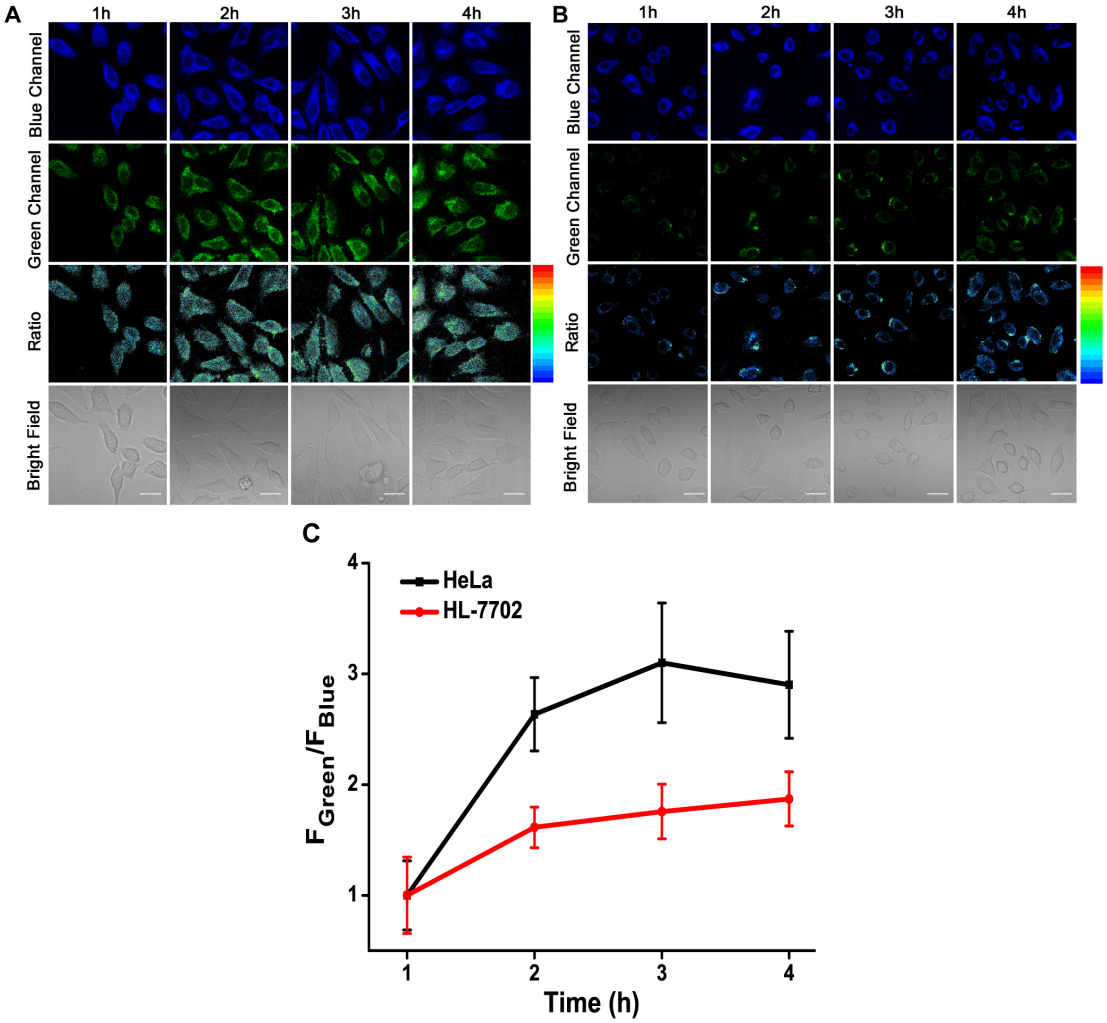

Figure S17. Fluorescence microscopy images of probe **ERNathS** (20 μM) in living cells (HeLa and HL-7702) for different time. (A) Images were acquired in HeLa cells after washing by PBS; (B) Images were acquired in HL-7702 cells after washing by PBS. Blue and green channel (425-475 nm, 500-550 nm), ratio images generated from green channel to blue channel. λ_{ex} = 405 nm. Scale bar: 20 μm. (C) The relative ratio value of fluorescence intensity (F_{Green}/F_{Blue}) in (A) and (B). Data represent mean standard error (n = 5).

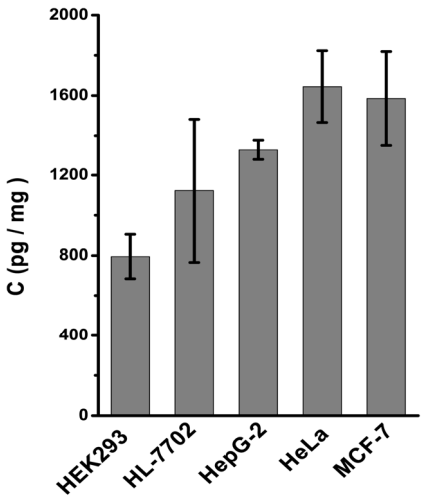

Figure S18. The concentrations of STS in the different cells (HEK-293 HL-7702, HepG-2, HeLa or MCF-7 cells) determined by an ELISA kit.

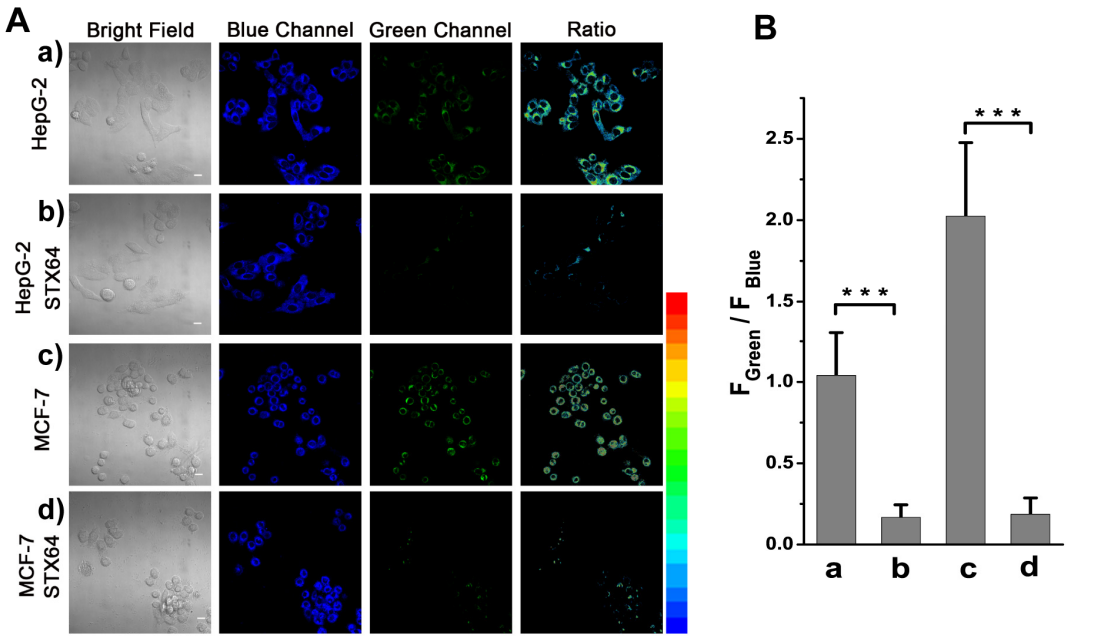

Figure S19. (A) Confocal microscopy images of HepG-2, MCF-7 cells incubated with probe **ERNathS** (20 μM) for 2 h: (a) HepG-2 cells, (b) HepG-2 cells pretreated 20 μM STX64 for 2 h, (c) MCF-7 cells, (d) MCF-7 cells pretreated with 20 μM STX64 for 2 h. Blue channel at 425-475 nm; Green channel at 500-550 nm; ratio images generated from green channel to blue channel. (B) The relative ratio value of the corresponding ratio images in panel A. Data represent mean standard error (n = 5). Statistical significance in A were calculated with unpaired two-tailed Student's t-tests.***p < 0.001, **p < 0.01. λ_{ex} = 820 nm. Scale bar: 20 μm.

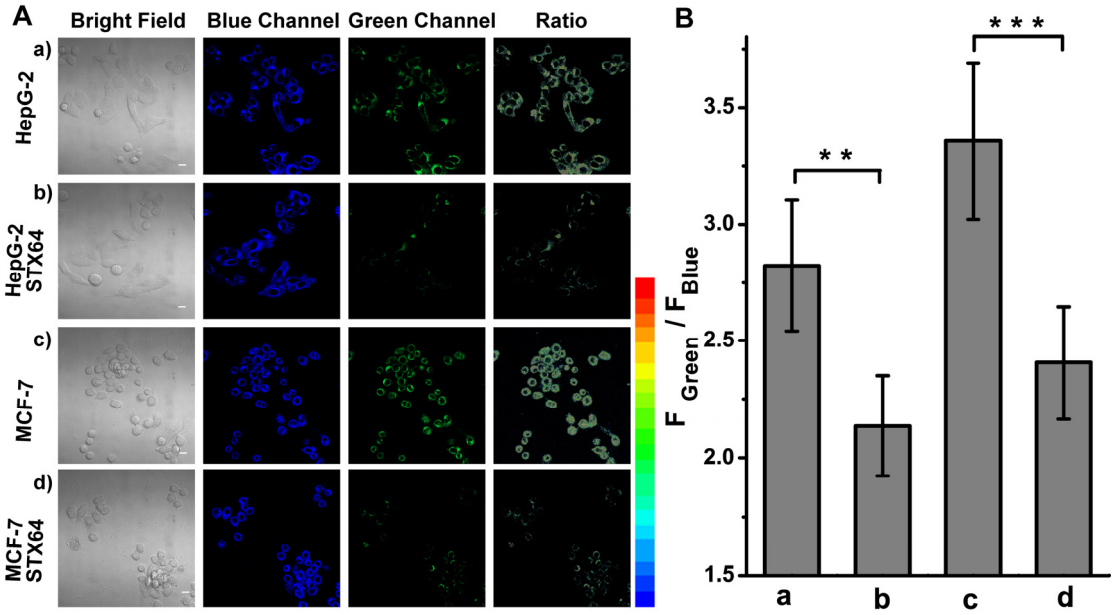

Figure S20. (A) Confocal microscopy images of HepG-2, MCF-7 cells incubated with probe **ERNathS** (20 μM) for 2 h: (a) HepG-2 cells, (b) HepG-2 cells pretreated 20 μM STX64 for 2 h, (c) MCF-7 cells, (d) MCF-7 cells pretreated with 20 μM STX64 for 2 h. Blue channel at 425-475 nm; Green channel at 500-550 nm; ratio images generated from green channel to blue channel. (B) The relative ratio value of the corresponding ratio images in panel A. Data represent mean standard error (n = 5). Statistical significance in A were calculated with unpaired two-tailed Student's t-tests.***p < 0.001, **p < 0.01. λ_{ex} = 405 nm. Scale bar: 20 μm.

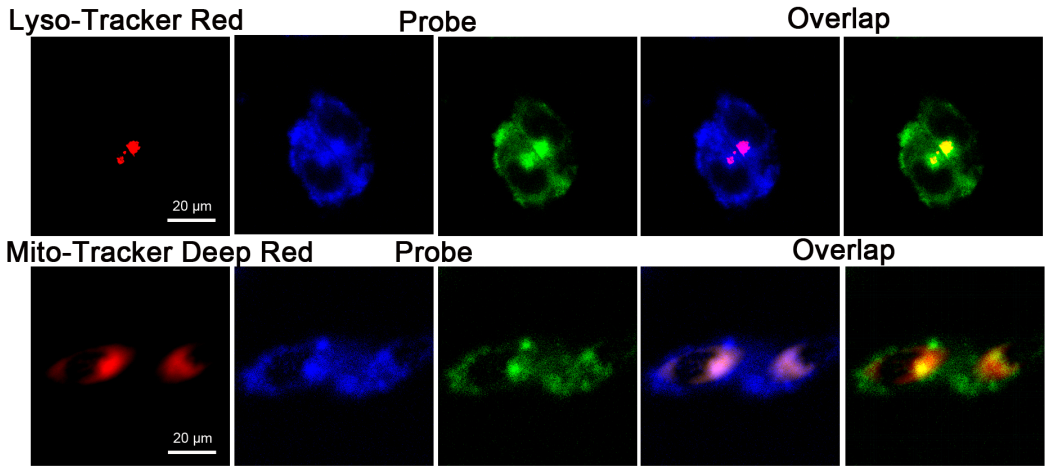

Figure S21. Measuring STS activity in subcellular organelle with **ERNathS**. Fluorescence of probe **ERNathS** (20 μM): Blue channel (425-475 nm) and Green channel (500-550 nm) with excitation 405 nm, Red channel: Lyso-Tracker Red (Excitation 561 nm, Emission 570-620 nm) and Mito-Tracker Deep Red (Excitation 640 nm, Emission 663-738 nm), respectively. Overlap: the merged signal. Scale bar: 20 μm.

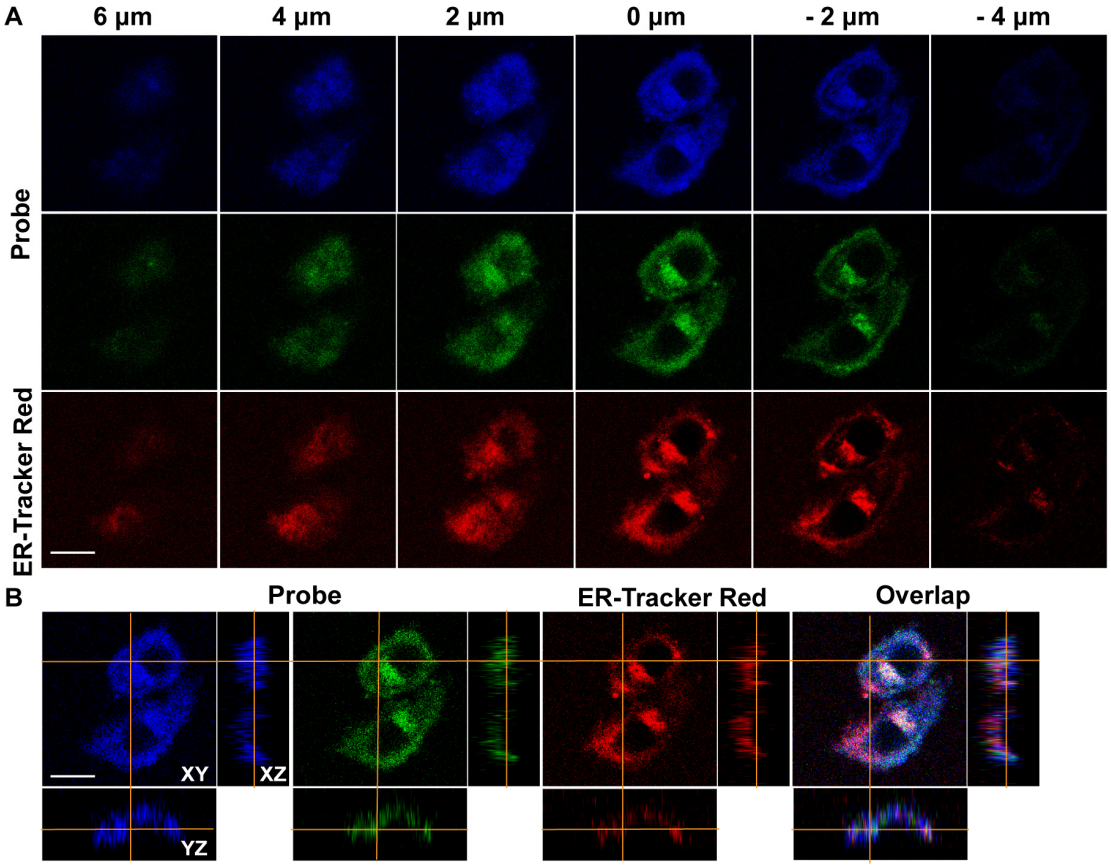

Figure S22. (A). Fluorescence images of z-direction slices of HepG-2 cells treated with probe **ERNathS** (20 μM) for 2 h followed by ER-Tracker Red for 20 min. (B). Confocal z-stacks images of (A) with a cross-section in xy, xz and yz. Fluorescence of probe **ERNathS**: Blue channel (425-475 nm) and Green channel (500-550 nm) with excitation 405 nm, ER-Tracker Red: Red channel (570-620 nm) with excitation 561 nm. Overlap: the merged signal. Scale bar: 20 μm.

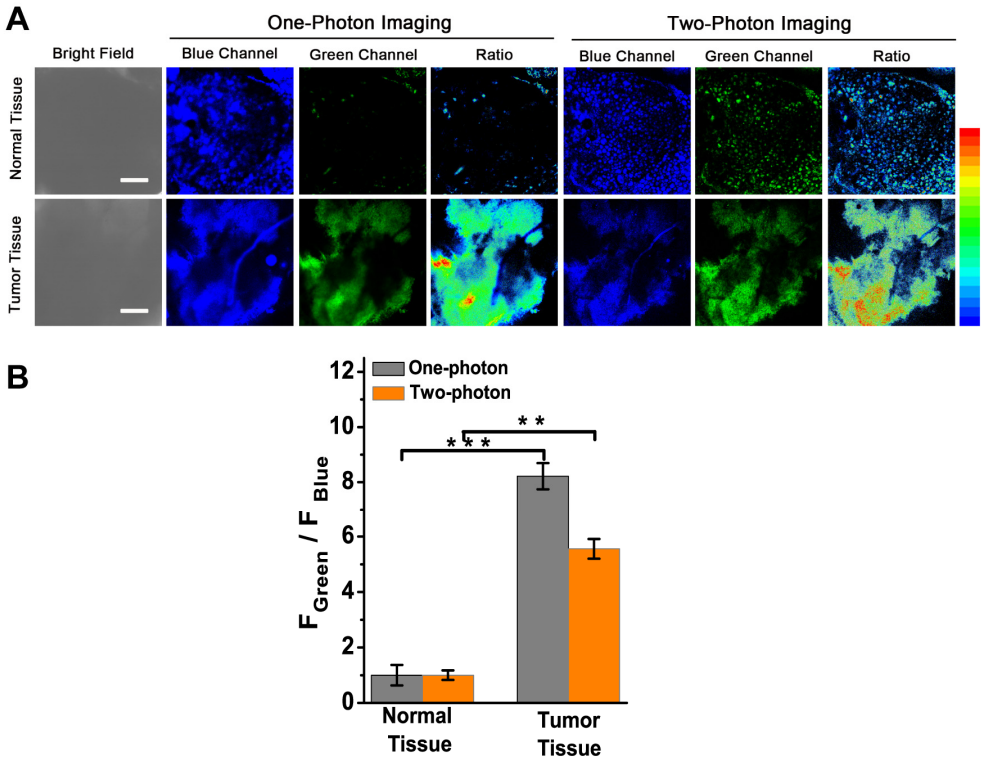

Figure S23. One-/two-photon fluorescence image of the normal and tumor tissues with a magnification of 10×. (A) The first row denotes the normal breast tissue, the second row denotes the tumor tissue; The one-photon mode (λ_{ex} = 405 nm) and the two-photon mode (λ_{ex} = 820 nm); (B) The relative ratio value of fluorescence intensity (F_{Green}/F_{Blue}) in panel (A). Data represent mean standard error (n = 3). Statistical significance in (A) were calculated with unpaired two-tailed Student's t-tests. **p < 0.01, ***p < 0.001. Blue channel (425-475 nm); Green channel (500-550 nm); ratio images generated from green channel to blue channel. Scale bar: 200 μm.

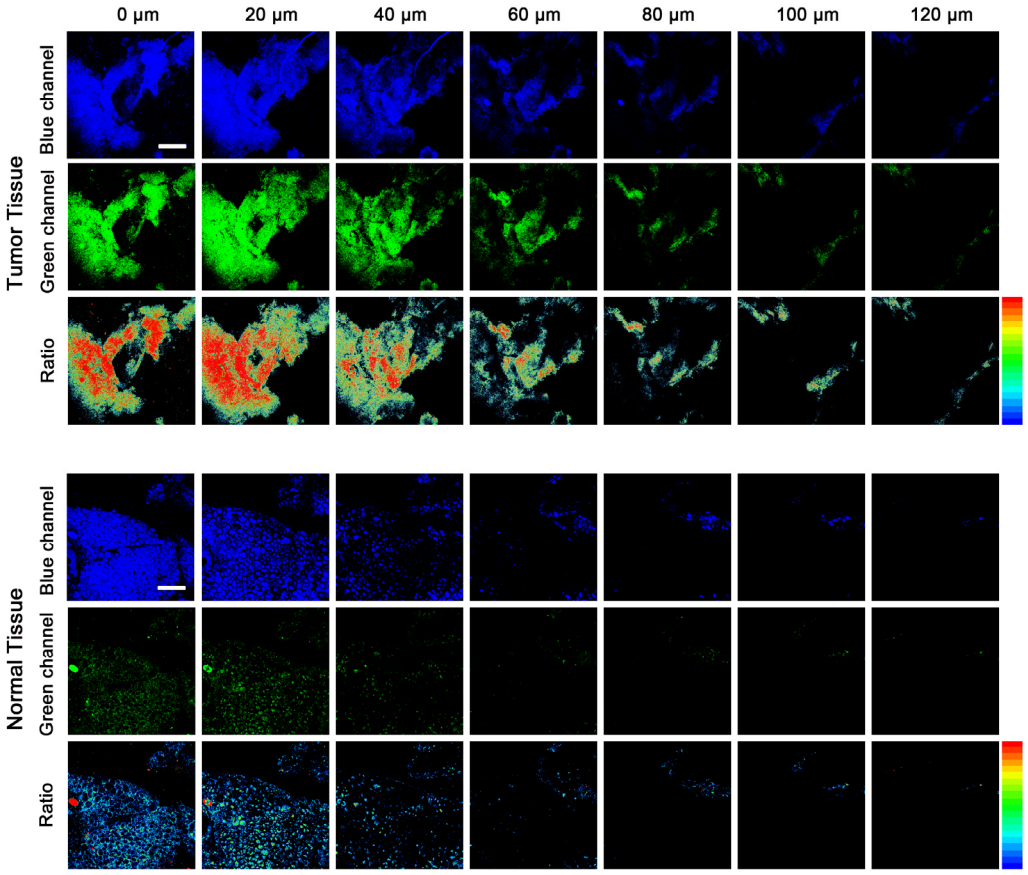

Figure S24. Depth fluorescence images of **ERNathS** with two-photon microscopy in the normal and tumor tissues. The changes of fluorescence intensity with scan depth were determined by spectral confocal microscopy (Nikon A 1 plus confocal microscope) in the z-scan mode (from -60 to 60 μm). Blue channel at 425-475 nm; Green channel at 500-550 nm; ratio images generated from green channel to blue channel. λ_{ex} = 820 nm. Scale bar: 200 μm.

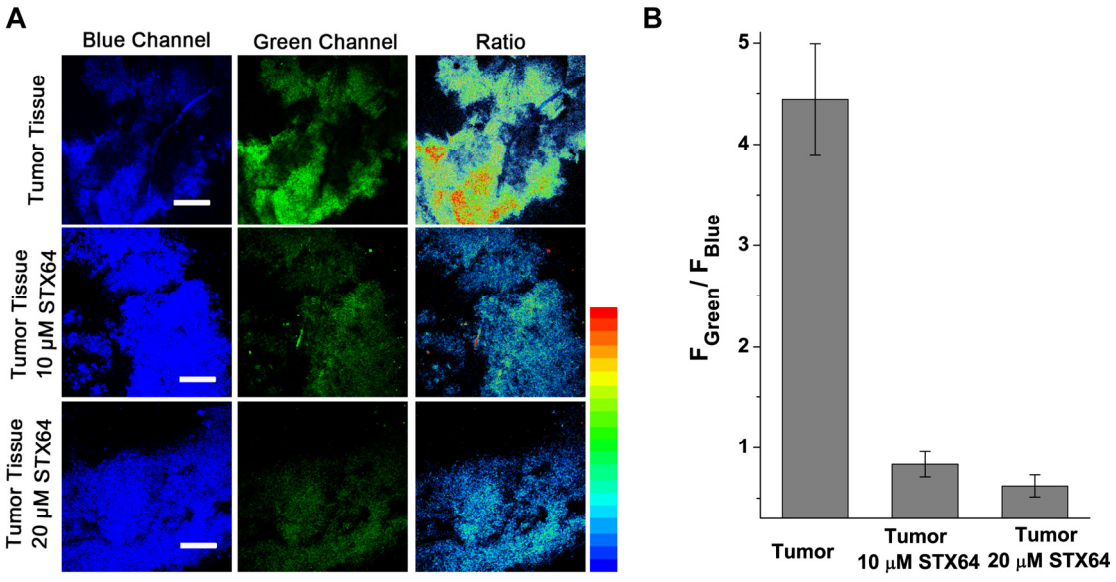

Figure S25. Two-photon fluorescence image of tumor tissues with a magnification of 10× under different concentration inhibitors STX64 (0, 10, 20 μM), Average ratio values of fluorescence intensity (F_{Green}/F_{Blue}) in panel (A). Data were expressed as mean ± standard deviation (SD) of three separate measurements. Blue channel at 425-475 nm; Green channel at 500-550 nm with the two-photon excitation wavelength at 820 nm; ratio images generated from green channel to blue channel. Data are expressed as mean ± SD of three parallel experiments. Scale bar: 200 μm.

5. Reference

1. R. F. Kubin and A. N. Fletcher, *J. Lumin.*, 1982, **27**, 455-462.
2. A. N. Fletcher and D. E. Bliss, *Appl. phys.*, 1978, **16**, 289-295.
3. N. S. Makarov, M. Drobizhev and A. Rebane, *Opt. Express*, 2008, **16**, 4029-4047.
4. T. Yanai, D. P. Tew and N. C. Handy, *Chem. Phys. Lett.*, 2004, **393**, 51-57.
5. R. Krishnan, J. S. Binkley, R. Seeger and J. A. Pople, *J. Chem.Phys.*, 1980, **72**, 650-654.
6. E. Runge and E. K. U. Gross, *Phys. Rev. Lett.*, 1984, **52**, 997-1000.
7. M. J. Frisch, G. W. Trucks, H. B. Schlegel, G. E.Scuseria, M. A. Robb, J. R. Cheeseman,G. Scalmani, V. Barone, B. Mennucci, G. A. Petersson et al. Gaussian 09, Revision A.1; Gaussian, Inc.: Wallingford, CT, 2009**.**
8. R. von Bülow, B. Schmidt, T. Dierks, K. von Figura and I. Usón, *J. Mol. Biol.*, 2001, **305**, 269-277.
9. H. Xiao, P. Li, X. Hu, X. Shi, W. Zhang and B. Tang, *Chem. Sci.*, 2016, **7**, 6153-6159.

6. NMR and MS spectra

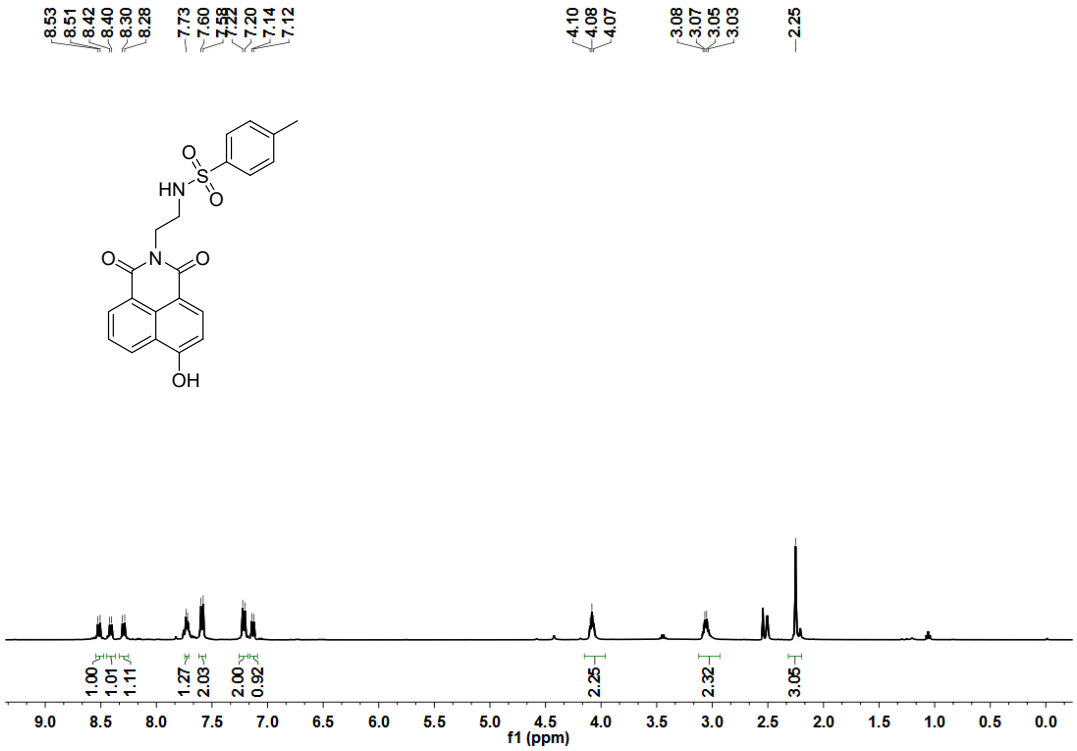

Figure S26. ^{1}H NMR spectrum of compound **ERNathOH.**

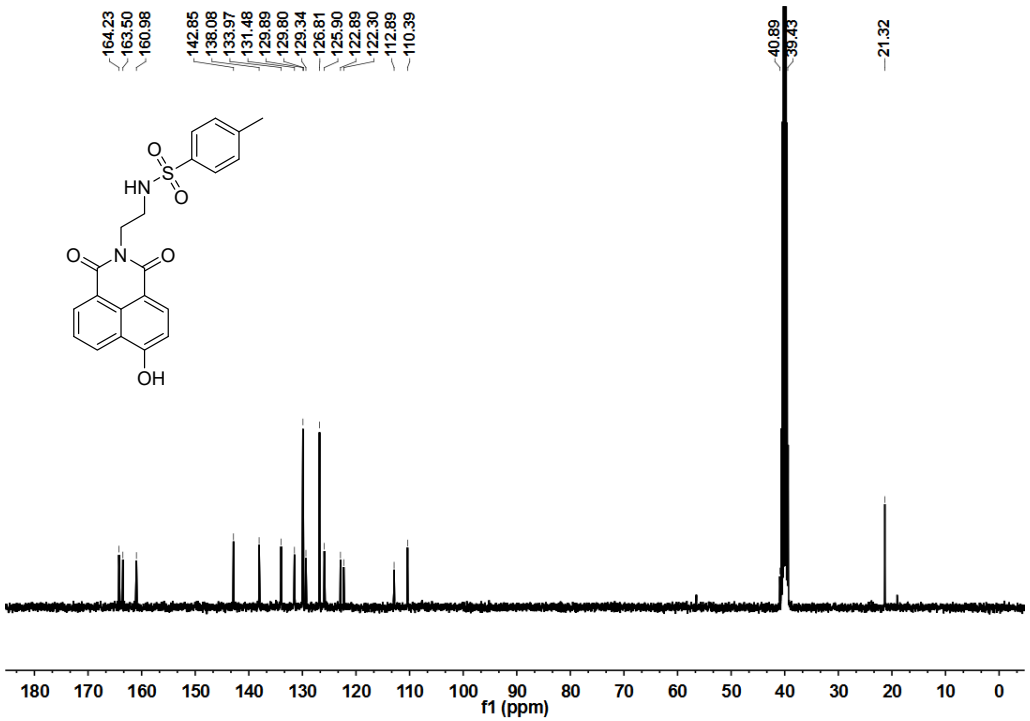

Figure S27. ^{13}C NMR spectrum of compound **ERNathOH.**

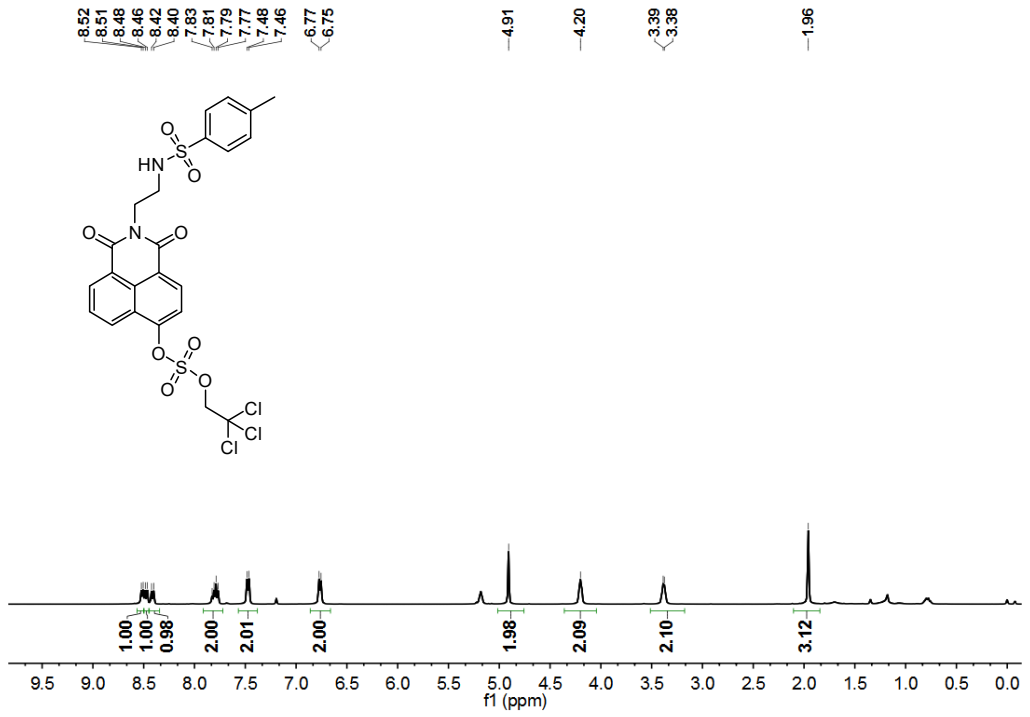

Figure S28. ^{1}H NMR spectrum of compound **ERNathS-Tce.**

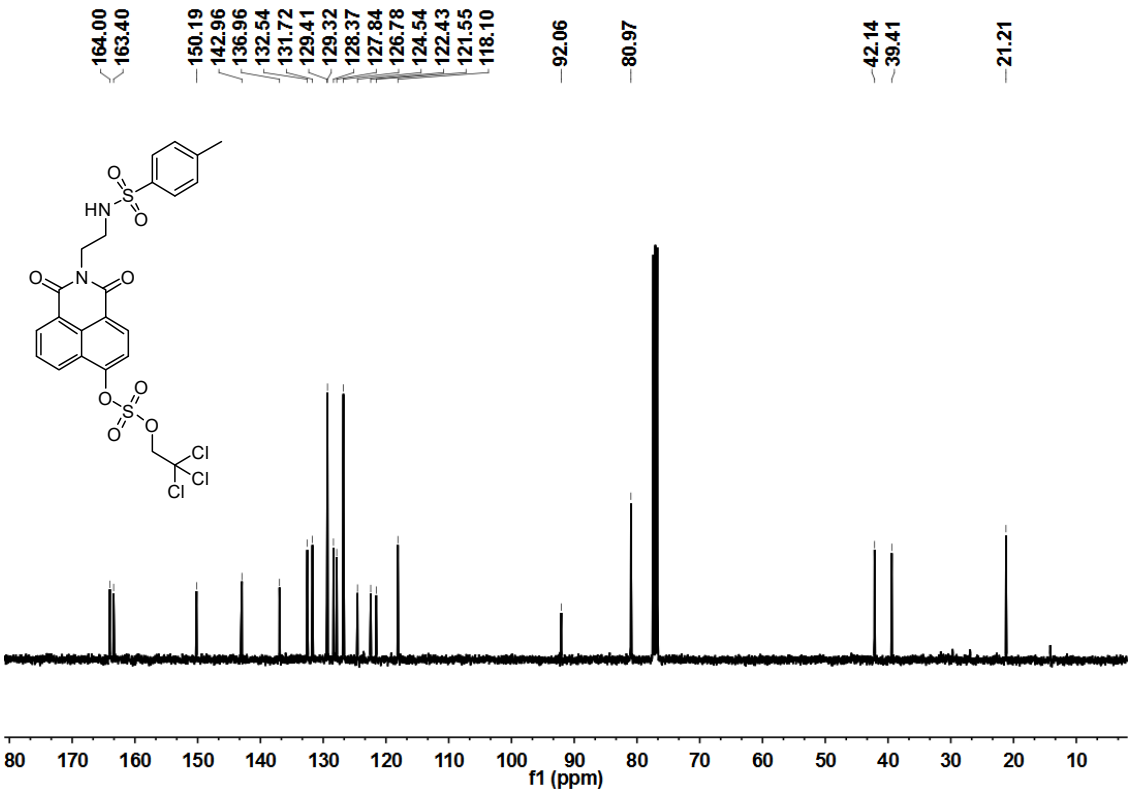

Figure S29. ^{13}C NMR spectrum of compound **ERNathS-Tce.**

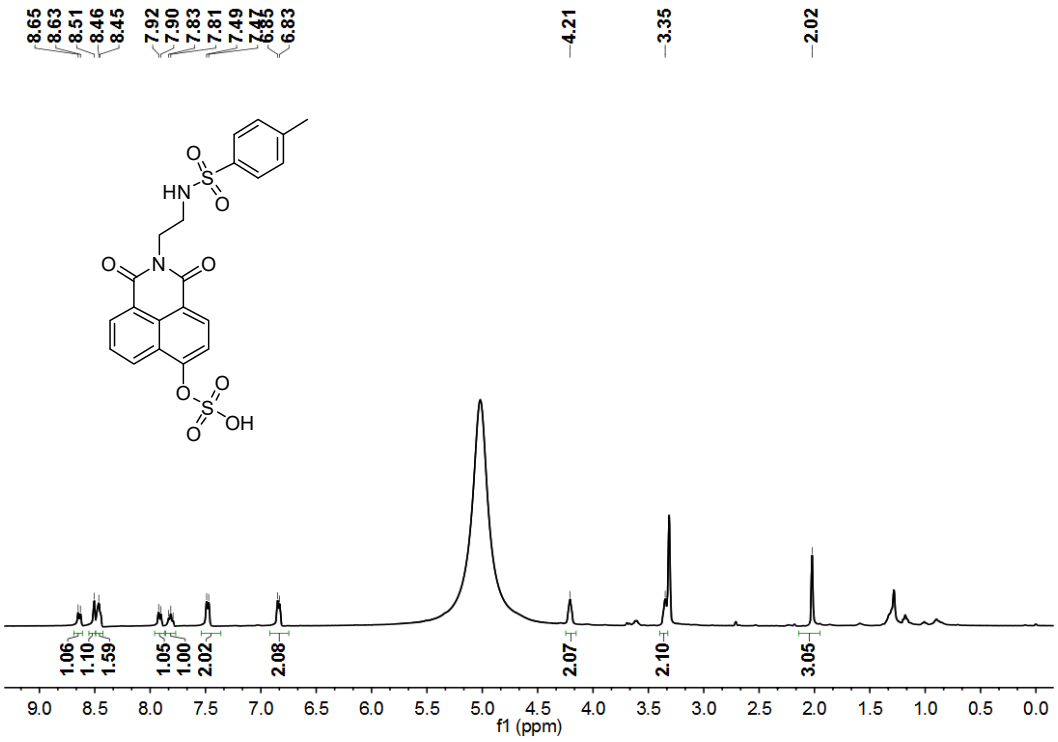

Figure S30. ^{1}H NMR spectrum of compound **ERNathS.**

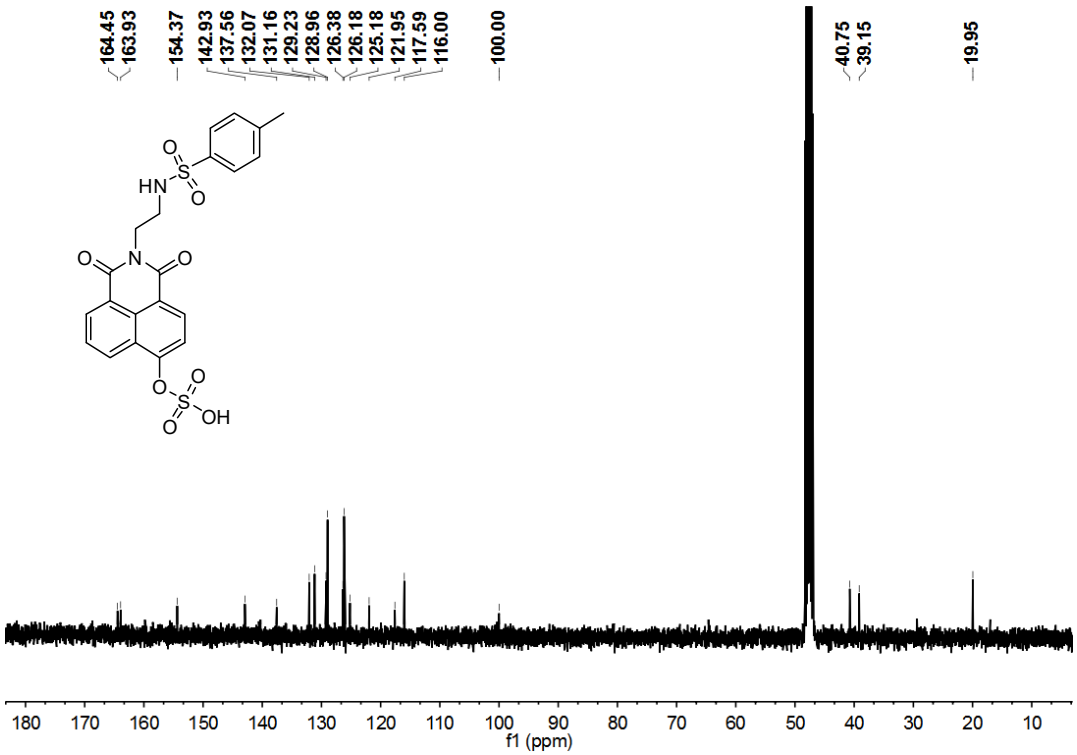

Figure S31. ^{13}C NMR spectrum of compound **ERNathS.**

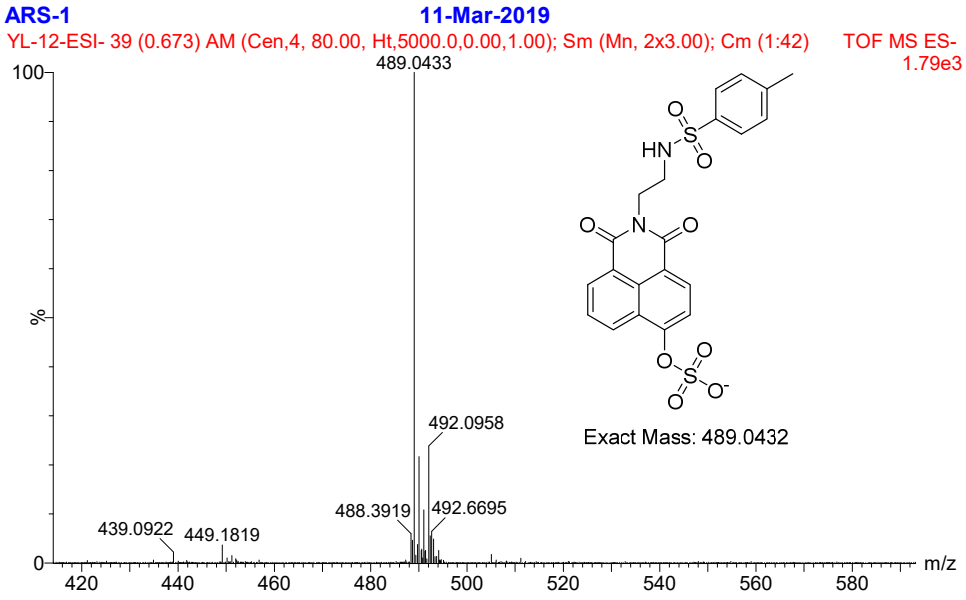

Figure S32. The HRMS spectra of **ERNathS**.